Prognostic relevance of adding MRI data to WHO 2016 and cIMPACT-NOW updates for diffuse astrocytic tumors in adults. Working toward the extended use of MRI data in integrated glioma diagnosis

Alexandre Roux, Stéphane Tran, Myriam Edjlali, Raphaël Saffroy, Arnault Tauziede-espariat, Marc Zanello, Albane Gareton, Edouard Dezamis, Frédéric Dhermain, Fabrice Chretien, et al.

Received: 11 August 2020 | Accepted: 14 December 2020

DOI: 10.1111/bpa.12929

Brain Pathology

RESEARCH ARTICLE

Prognostic relevance of adding MRI data to WHO 2016 and cIMPACT-NOW updates for diffuse astrocytic tumors in adults. Working toward the extended use of MRI data in integrated glioma diagnosis

Alexandre Roux[1,2,3] | **Stéphane Tran**[4] | **Myriam Edjlali**[2,3,5] | **Raphaël Saffroy**[6] | **Arnault Tauziede-Espariat**[2,3,4] | **Marc Zanello**[1,2,3] | **Albane Gareton**[2,4] | **Edouard Dezamis**[1,2,3] | **Frédéric Dhermain**[7] | **Fabrice Chretien**[2,3,4] | **Emmanuèle Lechapt-Zalcman**[2,3,4] | **Catherine Oppenheim**[2,3,5] | **Johan Pallud**[1,2,3] | **Pascale Varlet**[2,3,4]

[1]Service de Neurochirurgie, GHU Paris—Psychiatrie et Neurosciences—Hôpital Sainte-Anne, Paris, France

[2]Université de Paris, Sorbonne Paris Cité, Paris, France

[3]Inserm, UMR1266, IMA-Brain, Institut de Psychiatrie et Neurosciences de Paris, Paris, France

[4]Service de Neuropathologie, GHU Paris—Psychiatrie et Neurosciences—Hôpital Sainte-Anne, Paris, France

[5]Service de Neuroradiologie, GHU Paris—Psychiatrie et Neurosciences—Hôpital Sainte-Anne, Paris, France

[6]Service de Biochimie, Hôpital Paul-Brousse, AP-HP, Villejuif, France

[7]Département d'Oncologie Radiothérapie, Gustave Roussy Cancer Campus Grand Paris, Villejuif, France

Correspondence
Johan Pallud, Service de Neurochirurgie, Hôpital Sainte-Anne, 1, rue Cabanis, Paris Cedex 14 75674, France.
Email: johanpallud@hotmail.com

Funding information
Word carried out with the financial support of the AAIHP, www.aaihp.fr

Abstract

Assess the contribution of preoperative MRI data in improving grading of adult astrocytomas reclassified according to the WHO 2016 and cIMPACT-NOW update 3. Retrospective unicentric cohort study of 679 adult patients treated for newly diagnosed diffuse astrocytic and oligodendroglial tumors (January 2006–December 2016). We first systematically compared radiological (contrast enhancement present [CE+] vs. absent [CE−]) and histopathological findings (microvascular proliferation present [MPV+] vs. absent [MPV−]) to validate whether this comparing step of neoangiogenesis represents an efficient method to appreciate the representativity of the tumoral sampling. We focused on 629 cases of astrocytomas for radio-histological integrated analyses. In 598 cases (95.1%), neoangiogenesis evaluated by MRI or histology (CE+/MPV+ or CE−/MPV−) was identical. For the CE+/MPV− and CE−/MPV+ groups (23 cases), the radio-histological face-to-face evaluation allowed us to assess that for 13 cases (56.5%) the reason for this discrepancy was an undersampled tumor. We analyzed the group of CE+/MPV− (n = 8) and CE−/MPV+ (n = 2) in verified image-guided tumoral samples. Finally, we identified three new prognostic subgroups for molecular glioblastomas: (1) "non-representative sampling" (n = 9), (2) "Non neoangiogenic glioblastoma at the time of diagnosis, without contrast enhancement and microvascular proliferation" (n = 8), and (3) "contrast enhancing glioblastoma but without microvascular proliferation in a representative sample"

Alexandre Roux, Stéphane Tran, and Myriam Edjlali participated equally in this work.

Johan Pallud and Pascale Varlet participated equally in this work.

(n = 4). Neoangiogenesis processes should be assessed to improve the prognosis accuracy of the current integrated diagnosis. We suggest adding imaging analyses during the neuropathological analysis of astrocytomas in adults.

KEYWORDS
astrocytoma, histo-molecular, imaging, integrated diagnostics, WHO classification of CNS tumors

1 | INTRODUCTION

The classification of diffuse astrocytic and oligodendroglial tumors in adults has quickly evolved, thanks to major advances in molecular biology (1,2. Molecular diagnostic testing has become a mandatory addition to histo-immunophenotypical evaluation of gliomas in the 2016 update of the World Health Organization (WHO) classification of tumors of the central nervous system (CNS) (1. Therefore, no imaging criteria have been added for the assessment of diffuse glioma diagnosis and grading, except for diffuse midline glioma, *H3K27M*-mutant, for which precise tumor location is required (3.

For decades, the diagnostic approach for gliomas at Sainte-Anne hospital has involved a major step: establishing the tumor sample representativeness first. If the sample was not representative, grading was not formally established, and an alert on the risk of undergrading was given (4. The presence of microvascular proliferation and/or the presence of tumoral contrast enhancement (CE) on the preoperative MRI analysis had been shown to have a prognostic value on survival in oligodendrogliomas (5. In this line, the French Glioma Study Group confirmed in a large series of 927 grade II gliomas according to the 2007 WHO classification that a nodular-like pattern of CE and progressive CE over time, as opposed to faint and patchy patterns of CE, significantly impacted survival (6).

Again, adding MRI characteristics for glioma assessment and grading have generated contradictory data, difficult to compare, mainly caused by MRI technique differences and imaging evaluation criteria (7–10). To the best our knowledge, few study has correlated the MRI data in large series of gliomas reclassified according to 2016 WHO (7,11) but no study with the cIMPACT-NOW update 3 criteria (12) defining the "diffuse astrocytic glioma *IDH*-wild type with molecular features of glioblastoma." This new entity, regardless of its MRI aspect, describes an *IDH*-wild-type astrocytoma without morphological grade 4 criteria (microvascular proliferation and/or necrosis) but with molecular features of glioblastoma: (1) EGFR amplification, (2) combined gain of chromosome 7 and loss of chromosome 10, and/or (3) hTERT promoter mutation.

Here, we carried out a large cohort study of adult patients with glioma focusing on the prognostic impact of adding imaging data to the updated histomolecular data according to the 2016 WHO and to the cIMPACT-NOW update 3.

2 | MATERIALS AND METHODS

We performed a retrospective and consecutive cohort study of adult patients surgically treated for a newly diagnosed diffuse astrocytic and oligodendroglial tumors in a single institution at the Department of Neurosurgery, GHU Paris—Psychiatry and Neurosciences—Sainte-Anne Hospital—University of Paris, Paris, France, between January 2006 and December 2016. Inclusion criteria were: (1) hemispheric supratentorial location; (2) age ≥ 18 at diagnosis; (3) histopathological diagnosis of astrocytic, oligodendroglial, and oligoastrocytic tumors according to the 2007 WHO (13; (4) available clinical and follow-up data; (5) available preoperative Magnetic Resonance Imaging (MRI) performed in our institution; and (6) available histopathological material for neuropathological re-assessment. The methodology is detailed in Supporting Information.

2.1 | Clinical data

Clinical data were obtained from medical records by a neurosurgeon (AR) with subsequent validation by a second neurosurgeon (JP) while blind to imaging, histopathological, and molecular reviews. We used a specific form designed for the study, which was established by a neurosurgeon (JP), a neuropathologist (PV), and a neuroradiologist (MEG). Clinical data included: sex, age, first-line oncological treatment modalities including surgery, adjuvant therapies, oncological treatments at progression, progression-free survival, and overall survival. Progression-free survival was measured from the date of histopathological diagnosis to the date of evidence of progression or to the date of death. Tumor progression was defined according to the Response Assessment in Neuro-Oncology criteria in use at the time of management (14. Overall survival was measured from the date of histopathological diagnosis to the date of death from any cause. Surviving patients were censored at the date of last follow-up.

2.2 | Imaging parameters

Preoperative MRIs were performed at the time of the diagnosis using either a 1.5-T (Signa EchoSpeed; GE Healthcare, Milwaukee, Wis) or a 3.0-T (MR 750, GE Healthcare) MRI scanner. Contrast–enhanced 3D T1-weighted fast spoiled gradient-recalled acquisition (gadoterate meglumine [Dotarem; Guerbet, Aulnay-sous-Bois, France], 0.1 mmol/kg), axial 2D T1-weighted, and axial 2D FLAIR were analyzed. Imaging parameter data are available in Table 1.

2.3 | Independent radiological assessment

Imaging data were obtained from an independent central radiological review by two neuroradiologists (STB and MEG) while blind to clinical, histopathological, and molecular reviews, and outcomes.

Imaging data included: presence of a tumoral CE on preoperative MRI, which corresponds to a radiological neoangiogenesis, pattern of CE (faint and patchy, nodular, and ring-like) as previously described (6), and presence of necrosis.

2.4 | Independent histopathological assessment

We performed an independent neuropathological review of all cases by two neuropathologists (PV and ELZ) while blind to clinical and radiological reviews, and outcomes.

The first aim was to confirm the initial diagnosis of diffuse astrocytic and oligodendroglial tumors according to the WHO 2016 classifications including the cIMPACT-NOW update 3 (1,12,13 using additional immunostainings, if necessary. Neuropathological and molecular data included microvascular proliferation (MPV), necrosis, mitotic count, immunostatus for IDH1R132H and ATRX, 1p/19q-co-deletion status for suspected oligodendrogliomas, and results of targeted sequencing (*hTERT* promoter, *IDH1*, *IDH2*, *H3F3A*, *HIST1H3B*, and *BRAF*).

2.5 | Histo-radiological face-to-face consensus evaluation focused on the CE−/MPV+ and CE+/MPV− groups

After a second look, the criterion microvascular proliferation (MVP) (present/absent) was re-evaluated by pathologists (doubtful focal endothelial proliferation to MVP+ or MVP−). Neuroradiologists also re-evaluated the CE (present/absent) (doubtful CE) (Figure 1), including the detection of developmental venous anomaly, as previously described (15,16. The representativeness of the image-guided tissue sampling was assessed by matching preoperative MRI and early postoperative MRI (<48 h) for surgical resection or early postoperative CT-scan (<24 h) for biopsy to analyze the location of the surgically resected or biopsied area (Figure S1). For biopsy, we used the largest pneumocephalus bubble at the biopsy site to detect the surgical site. We checked in detail biopsy sites of CE+ tumors (inside or outside of contrast enhancing area) on preoperative MRI.

2.6 | Standard protocol approvals, registrations, and patient consents

This study was authorized by the French National Data Information and Freedom Commission (CNIL, reference number DE-2017–079) and the local ethics committee (CPP Ile-de-France 6, reference number n°2017-A02324–49, CPP/63–17).

TABLE 1 Magnetic resonance imaging sequence parameters

Parameters	GHU Paris––Psychiatry and Neurosciences––Sainte-Anne Hospital	
MR field	1.5 T	3 T
MR machine	GE Explorer	GE MR 750
FLAIR sequence		
TR/TE	8000/139 ms	10 000/190 ms
FOV	22 cm	22 cm
Slice thickness	3.5 mm	3.5 mm
Slice spacing	1.0 mm	0.5 mm
3D T1 with contrast		
TR/TE	10.2/3.4 ms	620/4.2 ms
FOV	24 cm	24 cm
Slice thickness	1.2 mm	1.2 mm
Slice spacing	0 mm	0 mm
Gadolinium dose	0.1 mmol/kg	0.1 mmol/kg

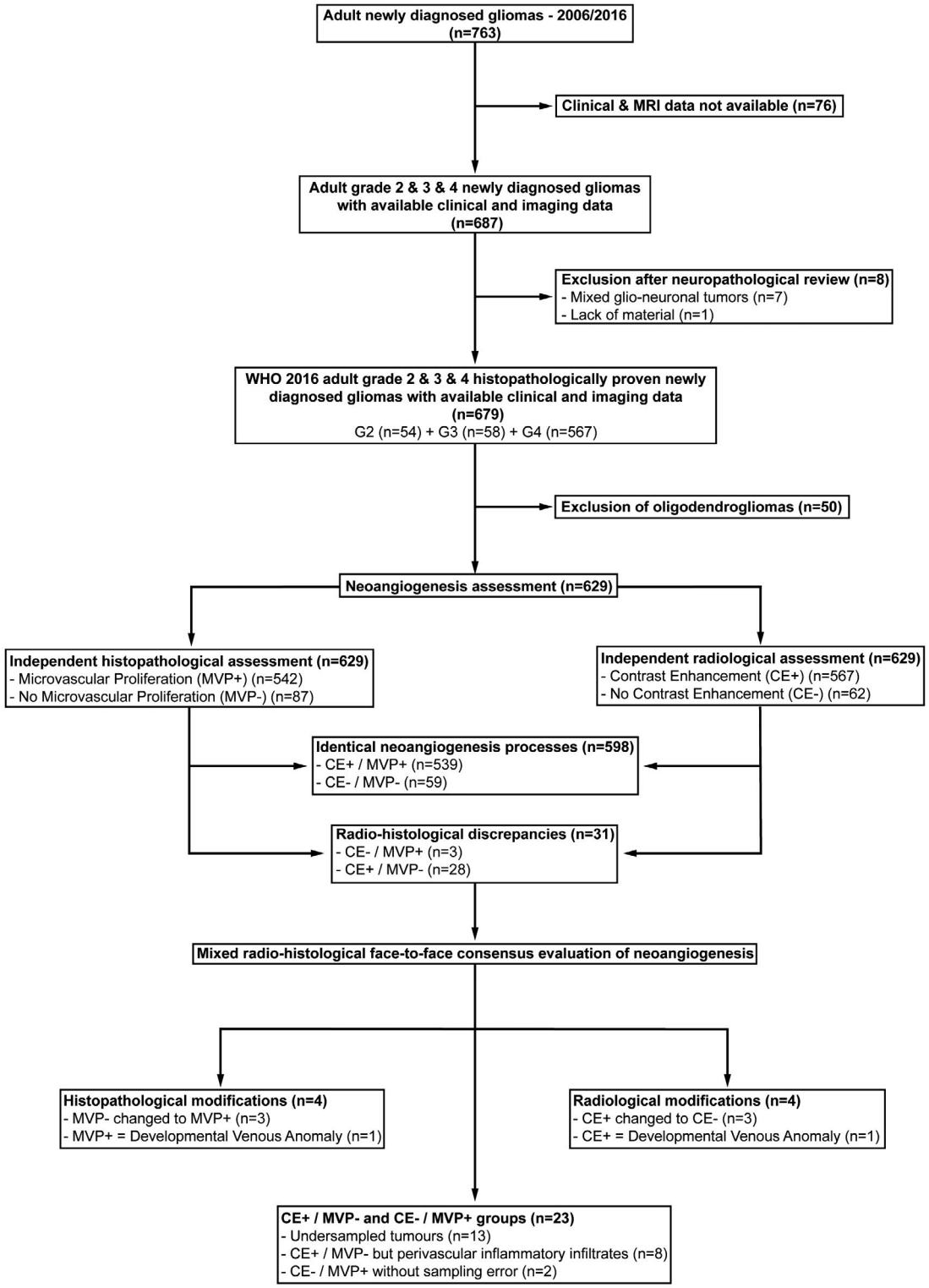

FIGURE 1 Patient flow chart

3 | RESULTS

3.1 | Patient characteristics

The patient flow chart is illustrated in Figure 1. A total of 679 patients (384 males, 56.6% and 295 females, 43.4%) were available for full analyses (54 grade 2 gliomas, 8.0%; 58 grade 3 anaplastic gliomas, 8.5%; and 567 grade 4 glioblastomas, 83.5%). Here, we decided to focus on astrocytomas for further analyses (n = 629). Main patient characteristics are detailed in Table S1. The median age at diagnosis was 60 years

Astrocytomas		Contrast Enhancement +	Contrast Enhancement -
Microvascular Proliferation	+	542	15
Microvascular Proliferation	-	8	64

FIGURE 2 Correlation analyses between microvascular proliferation and contrast enhancement (CE) for astrocytomas after consensus evaluation. Here, we described the correlation between the presence (+) or the absence (−) of microvascular proliferation and CE for astrocytomas after consensus evaluation

(range, 19–87) and 365 patients had a surgical resection (58.0%).

3.2 | Insights from the combined histo-radiological neoangiogenesis evaluation

For 598 cases (95.1%), angiogenesis evaluated by a histological criterion (MPV) or a radiological criterion (CE) was identical (539 CE+/MVP+ and 59 CE−/MVP−). For the other 31 cases (4.9%), the face-to-face histological and radiological evaluation found discrepancies (3 cases of CE−/MVP+ and 28 cases of CE+/MVP−).

These 31 cases, including 18 biopsies and 13 surgical resections, benefited from a re-assessment during a radio-histological consensus evaluation. Here, the criterion MVP (present/absent) was changed in four cases and the criterion CE (present/absent) was changed in four cases.

Four cases with CE+/MVP− were changed to CE−/MVP− with three cases related to a spontaneous hypersignal in T1 sequence and one case related to the presence of a developmental venous anomaly. One CE−/MVP+ case was changed to CE−/MVP− according to the misdiagnosis of MVP in context of developmental venous anomaly and three CE+/MVP− cases were changed to CE+/MVP+ according to the identification of a focal MVP.

Finally, we found 606 cases (96.3%) with identical neoangiogenesis processes including 542 CE+/MVP+ and 64 CE−/MVP−.

The two CE−/MVP+ remaining cases (with representative surgical samples) had only focal microvascular proliferation, which could explain the absence of CE on preoperative MRI. The vast majority of the 23 CE+/MVP− remaining cases were caused by 13 undersampled tumors. Finally, eight CE+/MVP− cases present a classical morphological aspect except the presence of a marked perivascular lymphocytic inflammatory infiltrates and a gemistocytic component (Figures 1 and 2).

The histo-radiological consensus evaluation is illustrated in Figure S1 and imaging data analyses are detailed in Table 2.

3.3 | Insights from an extended use of MRI data in the integrated astrocytoma diagnosis

Insights from the WHO 2007 and the WHO 2016 Classifications are detailed in Figures S2 and S3. Changes in subtypes and grading between the 2016 WHO Classification with the cIMPACT-NOW update 3 and integrative radio-histo-molecular assessment are illustrated in Figure 2.

The integrated radio-histo-molecular classification, focusing on astrocytomas and incorporating preoperative radiological analysis, allowed us to easily distinguish a group of classic glioblastoma whose diagnosis was finally carried out by the contribution of molecular criteria, but that could also have been done by a combined radio-histological evaluation.

The extended radio-histo-molecular integrated diagnosis refined the diagnosis of diffuse astrocytic glioma, *IDH*-wild type with molecular features of glioblastoma (n = 21) into three subgroups: (1) "non-representative sampling" (n = 9), (2) "Non neoangiogenic glioblastoma at the time of diagnosis, without CE and microvascular proliferation" (n = 8), and (3) "contrast enhancing glioblastoma but without microvascular proliferation in a representative sample" (n = 4). Interestingly, in all these cases, gemistocytic and/or perivascular lymphocytic inflammatory infiltrates were identified (Figure S1).

Four of the five cases of "non neoangiogenic" (CE−/MPV−) diffuse astrocytic glioma, *IDH*-wild type with molecular features of glioblastoma with available post-operative MRI follow-up (n = 5/8) had a ring-like CE, which appeared early during the follow-up (mean 4.3 months, range 1–9 months).

Finally, grade 3 anaplastic astrocytomas, *IDH*-wild type (n = 6) were reclassified as "non-representative sampling" (n = 2) and the remaining four cases have not been reclassified. Grade 3 anaplastic astrocytomas, *IDH*-mutant (n = 25) were reclassified as "non-representative sampling" (n = 3) and the remaining 22 cases have not been reclassified.

We found a higher rate of "non-representative sample" in the diffuse astrocytic glioma, *IDH*-wild type with molecular features of glioblastoma group (61.5%) than in grade 3 anaplastic astrocytoma, IDH-mutant (23.1%) than in grade 3 anaplastic astrocytoma, IDH-wild type (15.4%).

3.4 | Survival analyses

The median follow-up period was 64.9 months (range, 16.5–98.8) for grade 2 astrocytomas, 33.8 months (range, 0–112.8) for grade 3 anaplastic astrocytomas, and 15.2 months (range, 0–87.5) for grade 4 glioblastomas.

The progression-free survival and overall survival of patients according the 2016 WHO with the

TABLE 2 Imaging data analyses (n = 629)

Classification	Contrast enhancement n (%)	Type of contrast enhancement			Necrosis n (%)	Radio-histological discordances For neoangiogenesis processes
		Faint & patchy	Nodular	Ring-like		
WHO 2016 classification + cIMPACT-NOW updates						
Grade 2 astrocytomas, IDH-wild type	0/0 (0%)	0	0	0	0	0/0 (0%)
Grade 2 astrocytomas, IDH-mutant	3/32 (9.4%)	3	0	0	0	3/32 (9.4%)
Grade 3 anaplastic astrocytomas, IDH-wild type	2/6 (33.3%)	0	1	1	1	4/6 (66.7%)
Grade 3 anaplastic astrocytomas, IDH-mutant	5/25 (20.0%)	3	1	1	1	6/25 (24.0%)
Grade 4 glioblastomas, IDH-wild type	514/514 (100%)	31	67	416	416	514/514 (100%)
Grade 4 glioblastomas, IDH-mutant	24/28 (85.7%)	3	4	17	17	4/28 (14.3%)
Grade 4 diffuse midline gliomas, H3K27M-mutant	2/3 (66.7%)	0	0	2	2	0/3 (0%)
Grade 4 diffuse astrocytic gliomas, IDH-wild type, with molecular features of glioblastoma	13/21 (61.9%)	8	1	4	4	12/21 (57.1%)
Integrated radio-histo-molecular classification						
Grade 2 astrocytomas, IDH-wild type	0/0 (0%)	0	0	0	0	0/0 (0%)
Grade 2 astrocytomas, IDH-mutant	3/32 (9.4%)	3	0	0	0	3/32 (9.4%)
Grade 3 anaplastic astrocytomas, IDH-wild type	0/4 (0%)	0	0	0	0	2/4 (50.0%)
Grade 3 anaplastic astrocytomas, IDH-mutant	2/22 (9.1%)	2	0	0	0	3/22 (13.6%)
Grade 4 glioblastomas, IDH-wild type	514/514 (100%)	31	67	416	416	514/514 (100%)
Grade 4 glioblastomas, IDH-mutant	27/31 (87.1%)	4	5	18	18	7/31 (22.6%)
Grade 4 diffuse midline gliomas, H3K27M-mutant	2/3 (66.7%)	0	0	2	2	0/3 (0%)
Grade 4 glioblastoma *IDH*-wild type, with contrast enhancement but without microvascular proliferation in a representative sample	4/4 (100%)	4	0	0	0	4/4 (100%)
Nonrepresentative sampling of a grade 4 glioblastoma *IDH*-wild type	9/9 (100%)	4	1	4	4	8/9 (88.9%)
Grade 4 glioblastoma *IDH*-wild type, without contrast enhancement and microvascular proliferation	0/8 (0%)	0	0	0	0	0/8 (0%)

cIMPACT-NOW update 3, and the integrated radio-histo-molecular classification are presented in Table 3 and Figures 3–5 and Figure S4.

Out of the nine patients from the "non-representative sampling" in the diffuse astrocytic glioma *IDH*-wild type with molecular features of glioblastoma group, four received a standard chemoradiation protocol (Stupp regimen) as first-line adjuvant oncological treatment. However, three had only chemotherapy and two had only radiotherapy, which corresponds to undertreated patients.

The median overall survival was significantly longer in patients with "grade 4 glioblastoma *IDH*-wild type, with CE but without microvascular proliferation in a representative sample" (18.7 months), than patients with "grade 4 glioblastoma *IDH*-wild type, without CE and microvascular proliferation" (13.9 months), and than patients from the "non-representative sampling of a grade 4 glioblastoma *IDH*-wild type" (9.6 months) without reaching statistical significance ($p = 0.197$).

The median overall survival was significantly longer in the non-enhancing tumor subgroup (99.4 months) than in the faint and patchy CE subgroup (88.2 months) and the nodular and ring-like CE subgroup (13.5 months) ($p < 0.001$) (Figure 6). Similarly, the median progression-free survival was significantly longer in the non-enhancing tumor subgroup (33.9 months) than in the faint and patchy CE subgroup (23 months) and the nodular and ring-like CE subgroup (10 months) ($p < 0.001$) (Figure 6).

TABLE 3 Survival analyses according to the histopathological classification (n = 629)

		Progression-free survival			Overall survival		
Classification	n	Mean ± SD	Median	CI 95%	Mean ± SD	Median	CI 95%
WHO 2016 classification + cIMPACT-NOW updates							
Grade 2 astrocytomas, IDH-wild type	0	–	–	–	–	–	–
Grade 2 astrocytomas, IDH-mutant	32	34.5 ± 3.3	35.9	23.1–41.1	91.4 ± 3.8	98.8	nr–nr
Grade 3 anaplastic astrocytomas , IDH-wild type	6	29.6 ± 15.9	21.4	2.5–73.3	28.3 ± 17.0	8.1	0–105.4
Grade 3 anaplastic astrocytomas, IDH-mutant	25	34.9 ± 6.4	30.5	7.7–58.8	57.7 ± 4.7	70.8	60.8–nr
Grade 4 glioblastomas, IDH-wild type	514	13.1 ± 0.6	10.0	9.0–11.0	18.9 ± 1.0	13.5	12–15.9
Grade 4 glioblastomas, IDH-mutant	28	32.0 ± 5.5	23.0	17.0–35.3	56.6 ± 6.7	47.0	35.3–nr
Grade 4 diffuse midline gliomas, H3K27M-mutant	3	4.5 ± 3.6	4.5	0.9–8.0	5.3 ± 3.1	2.9	1.7–11.4
Grade 4 diffuse astrocytic gliomas, IDH-wild type, with molecular features of glioblastoma	21	11.8 ± 2.7	8.0	4.9–9.8	17.6 ± 3.5	12.2	7.3–23.1
Integrated radio-histo-molecular classification							
Grade 2 astrocytomas, IDH-wild type	0	–	–	–	–	-	–
Grade 2 astrocytomas, IDH-mutant	32	34.5 ± 3.3	35.9	23.1–41.1	91.4 ± 3.8	98.8	nr–nr
Grade 3 anaplastic astrocytomas, IDH-wild type	4	38.6 ± 18.5	32.6	10.1–73.3	41.1 ± 23.6	29.0	1.0–105.4
Grade 3 anaplastic astrocytomas, IDH-mutant	22	39.7 ± 7.1	33.9	4.6–64.9	61.2 ± 5.0	nr	60.8–nr
Grade 4 glioblastomas, IDH-wild type	514	13.1 ± 0.6	10.0	9.0–11.0	18.9 ± 1.0	13.5	12.0–15.9
Grade 4 glioblastomas, IDH-mutant	31	30.2 ± 4.9	23.0	14.0–35.3	53.9 ± 6.0	47.0	35.3–88.2
Grade 4 diffuse midline gliomas, H3K27M-mutant	3	4.5 ± 3.6	4.5	0.9–8.0	5.3 ± 3.1	2.9	1.7–11.4
Grade 4 diffuse astrocytic gliomas, IDH-wild type, with molecular features of glioblastoma and without microvascular proliferation	4	17.6 ± 7.4	11.0	8.8–39.6	26.4 ± 10.4	18.7	11.3–56.8
Periphery of grade 4 glioblastomas, IDH-wild type	11	10.6 ± 3.9	7.2	2.5–9.2	11.2 ± 3.8	9.6	0–18.8
Early-stage grade 4 glioblastomas, IDH-wild type	8	7.8 ± 3.3	4.8	3.0–24.0	16.3 ± 4.9	13.9	16.0–19.1

Abbreviations: CI 95%, 95% confidence interval; nr: not reached; SD: Standard deviation.

4 | DISCUSSION

4.1 | Key results

Herein, we report a large study of 629 astrocytomas in adults with an independent radio-histo-molecular central review, reclassified according to the 2016 WHO classification incorporating cIMPACT-NOW update 3 followed by a combined radio-histological consensus to assess the practical value of an extended use of MRI data in the integrated diagnosis.

First, we confirmed that the 2016 WHO classification incorporating cIMPACT-NOW update 3 presented a higher prognostic value than the 2016 WHO classification, reinforcing the discriminative importance of the selected histo-molecular characteristics, as suggested by a previous study (17.

Second, the *combined radio-histological neoangiogenesis evaluation was* concordant in 96.3%, proving that this simple step is efficient for the evaluation of the representativity of the tumor sample.

Third, we expanded the present knowledge identifying that diffuse astrocytic glioma, *IDH*-wild type with molecular features of glioblastoma according to cIMPACT-NOW update 3 encompasses three prognostic subgroups: (1) nonrepresentative sampling of a grade 4 glioblastoma *IDH*-wild type (CE+/MPV−), which corresponded to a surgical sampling located on the periphery of a contrast-enhancing area (42.9% of cases; median overall survival of 9.6 months). This group does not appear biologically and prognostically different from classical glioblastomas, IDH-wild type. The only diagnostic difficulty concerns neuropathological analysis (MPV− without necrosis) caused by the non-representativeness of the surgical samples. In these cases, the establishment of the adequate diagnosis can, therefore, be carried out as well by adding the molecular data but also by adding the basic MRI data. Preoperative imaging is very often available as part of the minimum presurgical evaluation. (2) "Non angiogenic glioma" at the time of diagnosis (CE−, MPV− with an imaged-guided representative sample) (38.1% of cases; median overall survival of 13.9 months).

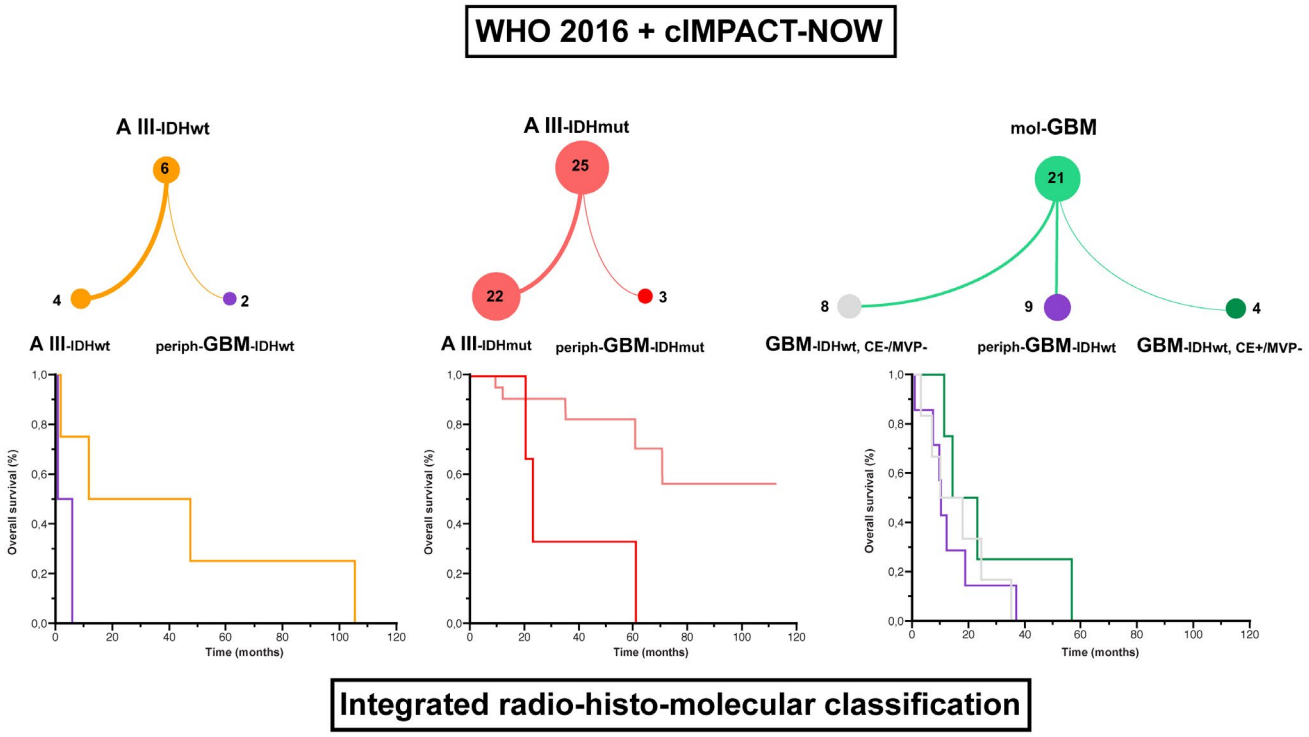

FIGURE 3 Diagnosis and grade changes from 2016 WHO Classification with cIMPACT-NOW updates to integrative radio-histo-molecular assessment. *Integrated radio-histo-molecular classification*. AIII-*IDH*mut: grade 3, anaplastic astrocytoma, *IDH*-mutant; AIII-*IDH*wt: grade 3, anaplastic astrocytoma, *IDH*-wild type; mol-GBM: diffuse astrocytic glioma, *IDH*-wild type, with molecular features of glioblastoma ; periph-GBM-*IDH*mut: periphery of grade IV, glioblastoma, *IDH*-mutant; periph-GBM-*IDH*wt: periphery of grade IV, glioblastoma, *IDH*-wild type; GBM-*IDH*wt, CE−, MVP−: grade 4 glioblastoma *IDH*-wild type, without contrast enhancement (CE) and microvascular proliferation; GBM-*IDH*wt, CE+, MVP−: grade 4 glioblastoma *IDH*-wild type, with CE but without microvascular proliferation in a representative sample. Kaplan–Meier estimates of overall survival (OS) according to our integrated radio-histo-molecular classification. Concerning AIII-*IDH*wt (left), the median OS was longer in patients with AIII-*IDH*wt (29 months) than patients with periph-GBM-*IDH*wt (2.6 months), without reaching statistical significance ($p = 0.107$). Concerning AIII-*IDH*mut (middle), the median OS was significantly longer in patients with AIII-*IDH*mut (not reached) than patients with periph-GBM-*IDH*mut (23.1 months) ($p = 0.010$). Concerning mol-GBM (right), the median OS was longer in patients with GBM-*IDH*wt, CE+, MVP− (18.7 months), than patients with GBM-*IDH*wt, CE−, MVP− (13.9 months), and than patients with periph-GBM-*IDH*wt (9.6 months), without reaching statistical significance ($p = 0.197$)

These astrocytomas can develop CE areas early during the follow-up (80.0% of cases in our study). These tumors could correspond to the "early-stage glioblastoma," as described by Ideguchi et al (18. In our cohort, they paradoxally had a poorer survival rate and rather represent fast growing tumors. (3) A very rare situation, "grade 4 glioblastoma *IDH*-wild type, with CE but without microvascular proliferation in a representative sample" (19.0%; median overall survival of 18.7 months) in which the CE could not be explained by microvascular proliferation but instead by marked perivascular lymphocytic infiltrates. Interestingly, all of these cases included a morphological gemistocytic tumoral component, a well described association (19. However, to date, no study has demonstrated that a perivascular lymphocytic infiltrate could on its own create a CE.

Finally, we confirmed that the pattern of CE observed on preoperative MRI (no CE, faint and patchy, nodular and ring-like) significantly impacts overall survival, as previously described (6. The ring-like and nodular patterns of CE were associated with a lower overall survival rate, which highlights its usefulness as an easily available prognostic marker in an integrated grading system.

4.2 | Interpretation

Tumoral sampling representativity, which is reached in 98% of the cases in our study, is frequently mentioned in pathology (20 but it is rarely integrated into the diagnostic process in daily clinical neuropathology practice. The variable proportion of these sampling biases could partly explain the variability of the percentage of contrast enhancing tumors, in different subtypes and grades of astrocytomas, which are a hallmark of aggressiveness. Delfanti *et al*., found no significant difference in CE among 40 grade 2/3 oligodendrogliomas, *IDH*-mutant, and *IDH*-wild-type astrocytomas but none of these tumors demonstrated marked CE on MRI (7. The absence of CE was also predictive of longer progression-free survival in series of gliomas reclassified according to the 2016 WHO

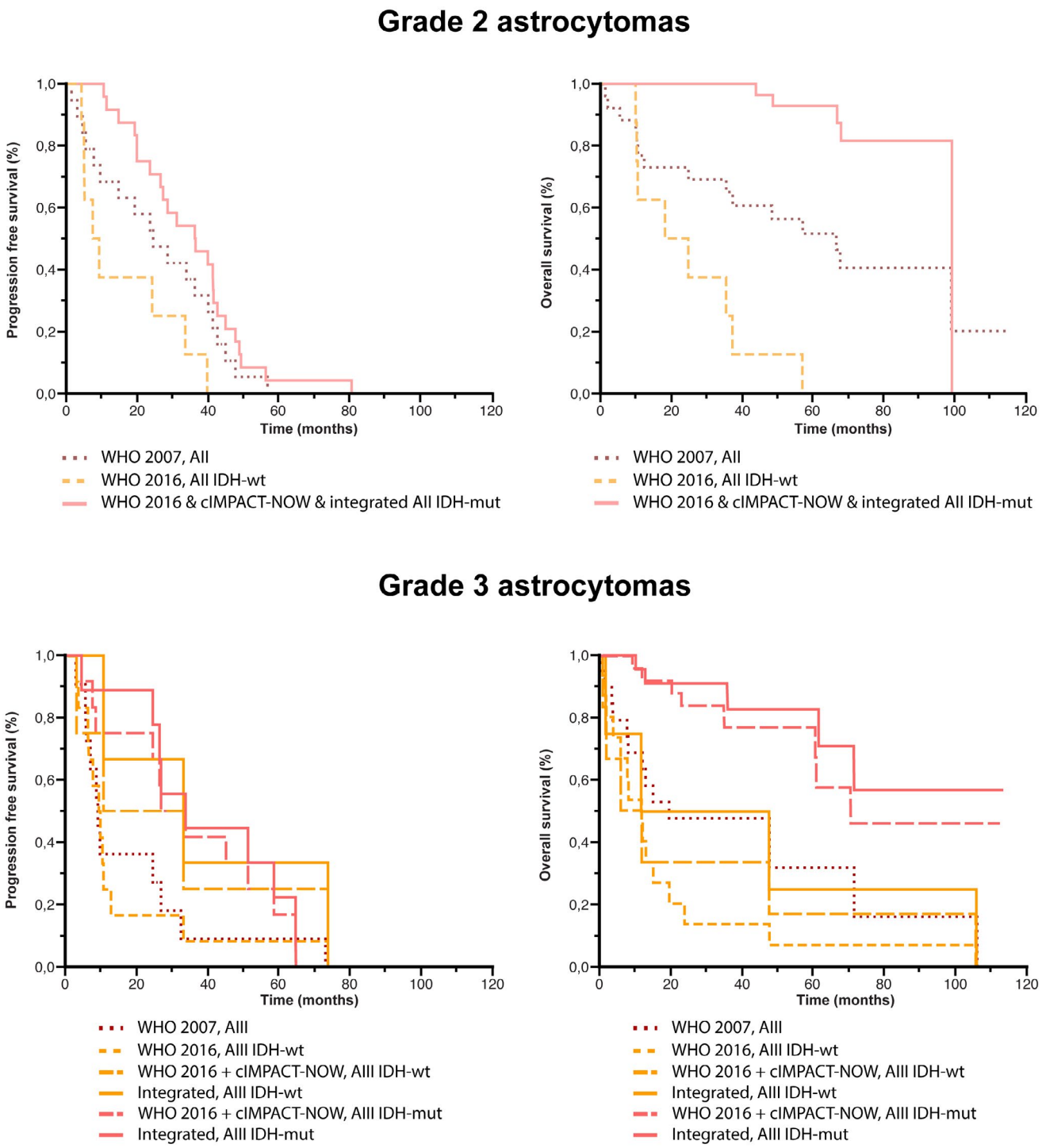

FIGURE 4 Comparison of survival analyses in astrocytomas according to the classifications used. Kaplan–Meier estimates of progression-free survival (PFS) and OS for astrocytomas according to histo-molecular classifications. Concerning Grade 2 astrocytomas, the median PFS and OS were longer in patients with AII-*IDH*mut (WHO 2016 classification with cIMPACT-NOW update 3 and our integrated classification) (35.9 and 98.8 months, respectively), than in patients with AII (WHO 2007 classification) (24.0 and 66.3 months, respectively), and than in patients with AII-*IDH*wt (WHO 2016 classification) (8.1 and 21.2 months, respectively). Concerning Grade 3 anaplastic astrocytomas, the median PFS was longer in patients with AIII-*IDH*mut (our integrated classification) (33.9 months), than in patients with AIII-*IDH*wt (our integrated classification) (32.6 months), than in patients with AIII-*IDH*mut (WHO 2016 classification & WHO 2016 classification with cIMPACT-NOW update 3) (30.5 months), than in patients with AIII-*IDH*wt (WHO 2016 classification with cIMPACT-NOW update 3) (21.4 months), than in patients with AIII (WHO 2007) (9.2 months), and than in patients with AIII-*IDH*wt (WHO 2016 classification) (9.0 months). The median OS was longer in patients with AIII-*IDH*mut (our integrated classification) (not reached), than in patients with AIII-*IDH*mut (WHO 2016 classification & WHO 2016 classification with cIMPACT-NOW update 3) (70.8 months), than in patients with AIII-*IDH*wt (our integrated classification) (29.0 months), than in patients with AIII (WHO 2007) (18.8 months), than in patients with AIII-*IDH*wt (WHO 2016 classification) (11.0 months), than in patients with AIII-*IDH*wt (WHO 2016 classification with cIMPACT-NOW update 3) (8.1 months)

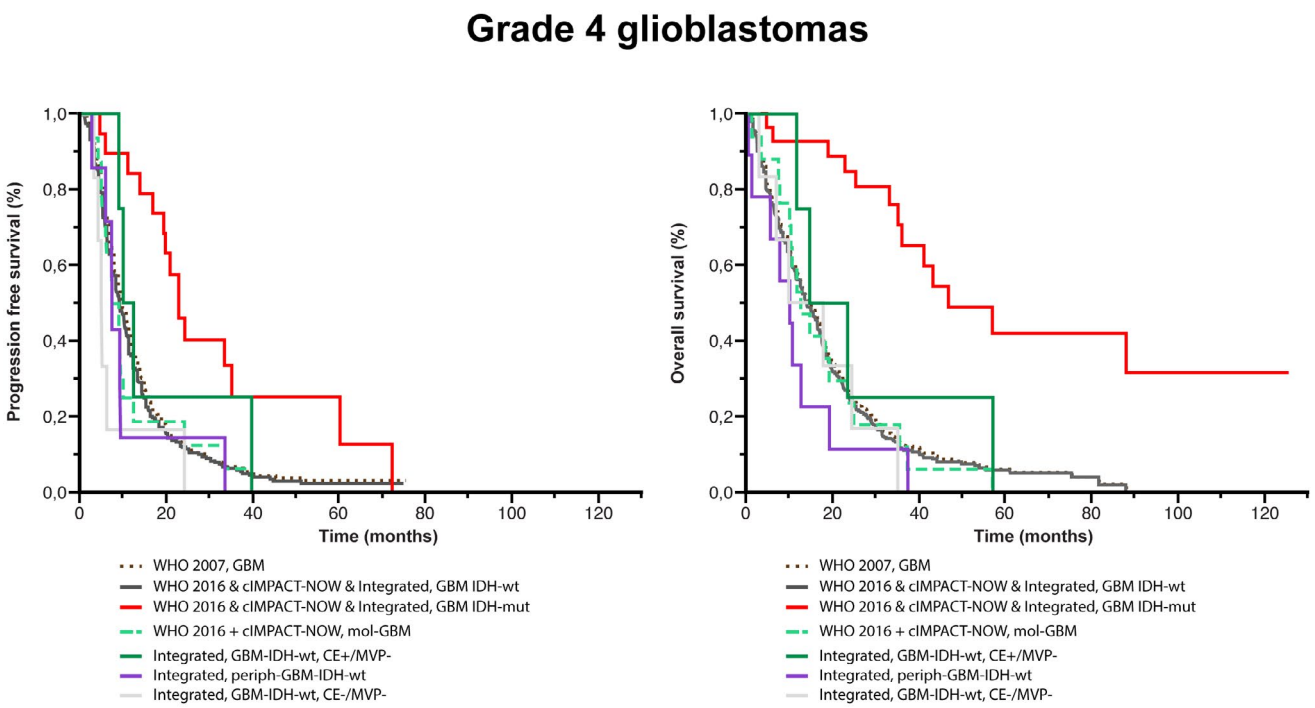

FIGURE 5 Comparison of survival analyses in glioblastomas according to the classifications used. Kaplan–Meier estimates of progression-free survival (PFS) and OS for glioblastomas according to histo-molecular classifications. The median PFS was longer in patients with GBM-*IDH*mut (WHO 2016 classification & WHO 2016 classification with cIMPACT-NOW update 3 & our integrated classification) (23.0 months), than in patients with GBM-IDHwt, CE+/MVP− (our integrated classification) (11.0 months), than in patients with GBM (WHO 2007 classification) (10.0 months) or patients with GBM-*IDH*wt (WHO 2016 classification & WHO 2016 classification with cIMPACT-NOW update 3 & our integrated classification) (10.0 months), than in patients with mol-GBM (WHO 2016 classification with cIMPACT-NOW update 3) (8.0 months), than in patients with periph-GBM-*IDH*wt (our integrated classification) (7.2 months), and than in patients with GBM-IDHwt, CE−/MVP− (6.0 months). The median OS was longer in patients with GBM-*IDH*mut (WHO 2016 classification & WHO 2016 classification with cIMPACT-NOW update 3 & our integrated classification) (47.0 months), than in patients with GBM-IDHwt, CE+/MVP− (our integrated classification) (18.7 months), than in patients with GBM-IDHwt, CE−/MVP− (14.5 months), than in patients with GBM (WHO 2007 classification) (14.4 months), than in patients with GBM-*IDH*wt (WHO 2016 classification & WHO 2016 classification with cIMPACT-NOW update 3 & our integrated classification) (13.5 months), than in patients with mol-GBM (WHO 2016 classification with cIMPACT-NOW update 3) (12.2 months), and than in patients with periph-GBM-*IDH*wt (our integrated classification) (9.6 months)

classification (10,21. Otherwise, in grade 3 anaplastic gliomas, *IDH*-mutant, CE seems to be associated with a worse survival outcome (22. The integration step allows us to detect a limited number of nonrepresentative samples in our cohort (n = 15, 2.2%). Recently, Hasselblatt *et al.* reclassified 212 grade 2 diffuse astrocytomas, according WHO 2016 and excluded 44 contrast-enhancing cases, which represented a significant proportion of nonrepresentative surgical samples (20%) (23. These comparative data in each molecular subgroup associated to the "corrected step" of sampling evaluation were analyzed, as well as how they related to patient survival. We also assessed whether the representative stage improves the prognostic value of the grade or could replace the integration of more sophisticated and expensive biomarkers, particularly in centers or countries with limited resources (24).

Here, integrating imaging into histo-molecular analyses helps in refining survival data for glioma patients. This method of making a diagnosis, without questioning WHO 2016, but by simply adding conventional MRI data for the neuropathological analysis and for establishing the neuropathological report, allows us to discriminate between these three prognostic groups in the recently described diffuse astrocytic glioma, *IDH*-wild type with molecular features of glioblastoma. We underline the interest of a radiological analysis during the realization of the neuropathology report in order to take into account the representativity of surgical sampling in the final diagnosis.

The concept of "non angiogenic" grade 4 glioblastoma, *IDH*-wild type is defined radiologically as small abnormal signal intensity on FLAIR sequences without CE detected by an MRI performed early in the course of the disease (18,25,26. This concept has been described earlier than cIMPACT-NOW update 3, and to the best of our knowledge, no initial and serial data describing detailed MRI results in a molecular glioblastoma series are yet available. In our series, grade 4 glioblastoma *IDH*-wild type, without CE and microvascular proliferation are molecularly similar to classic glioblastoma, *IDH*-wild type but present lower survival rates than classic grade 4 glioblastoma, *IDH*-wild type, which suggested either an early-stage at diagnosis or a fast-growing glioblastomas. However, in our study, we cannot

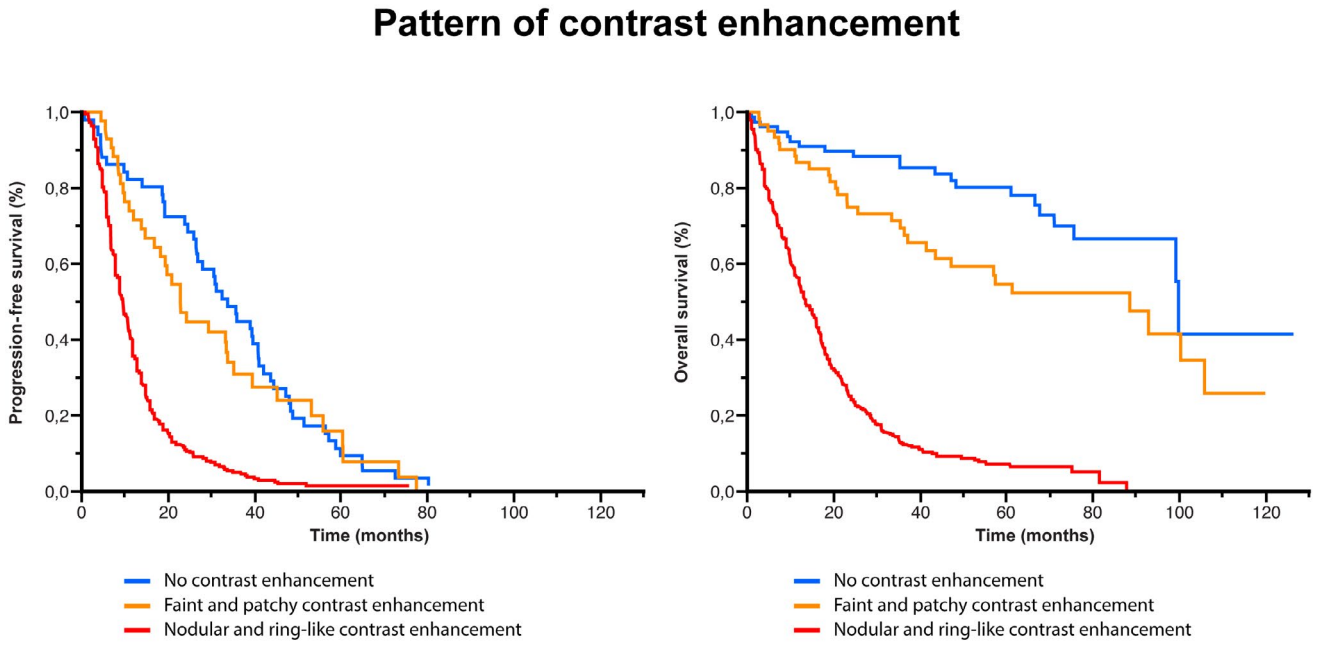

FIGURE 6 Comparison of survival analyses according to the pattern of contrast enhancement (CE). Kaplan–Meier estimates of PFS and OS according to the pattern of CE. The median PFS was significantly longer in the non-enhancing tumor subgroup (33.9 months) than in the faint and patchy CE subgroup (23 months) and the nodular and ring-like CE subgroup (10 months) ($p < 0.001$). The median OS was significantly longer in the non-enhancing tumor subgroup (99.4 months) than in the faint and patchy CE subgroup (88.2 months) and the nodular and ring-like CE subgroup (13.5 months) ($p < 0.001$)

exclude that the difficulties establishing the glioblastoma diagnosis on a lesion without CE could modify the achievement of the optimal treatment and influence the more unfavorable prognosis.

Finally, grade 4 glioblastoma *IDH*-wild type, with CE but without microvascular proliferation in a representative sample are very exceptional. The CE could not be explained by MPV but rather by the presence of a perivascular lymphocytic inflammatory infiltrates, which alters the blood–brain barrier (27,28. They could represent a subgroup of less aggressive glioblastomas with a frequent gemistocytic component.

4.3 | Generalizability

The present study suggests systematically carrying out a radiological assessment during neuropathological analysis in order to: (1) assess the tumoral sample representativeness to (2) propose an integrated radio-histo-molecular diagnosis of adult gliomas and, (3) improve the oncological management, especially for patients at risk of an undergrading, caused by an undersampled tumors.

4.4 | Limitations

The results should be interpreted with full knowledge of the exploratory and retrospective design of the study, which excluded patients based on lack of clinical data, imaging data, and/or tumor material. The design of this study, without an external validation set and a low number of patients in the new prognostic groups proposed, also limited the generalizability of the results. As a consequence, the clinical relevance of the predictors of postoperative outcomes remain to be confirmed by further investigations.

4.5 | Conclusion

We report a large study of 629 gliomas in adults with an independent radio-histo-molecular central review followed by a combined radio-histological face-to-face consensus evaluation of the neoangiogenesis processes to assess the importance of an integrated radio-histo-molecular classification at the era of the 2016 WHO Classification with cIMPACT-NOW updates. We demonstrated that combining MVP on histopathological analysis and CE on imaging represents an easy and effective step to assess undersampled tumors. Adding preoperative and postoperative imaging analyses to the current histo-molecular diagnosis in daily clinical practice seems to be promising. Multicentric studies will have to be carried out in order to clarify the place of imaging in the diagnosis of gliomas.

ACKNOWLEDGMENTS

Alexandre Roux would like to thank the *Nuovo-Soldati Foundation* for Cancer Research for their support.

CONFLICT OF INTEREST

The authors declare that they have no conflict of interest.

AUTHOR CONTRIBUTIONS

Data collection: AR, STB, ME, RS, ATE, ELZ, JP, and PV. *Data analysis:* AR, STB, ME, RS, ATE, ELZ, JP, and PV. *Data interpretation:* AR, STB, ME, RS, ATE, MZ, AG, ED, FD, FC, ELZ, CO, JP, and PV. *Report writing:* AR, STB, ME, RS, ATE, MZ, AG, ED, FD, FC, ELZ, CO, JP, and PV. *Proofreading and paper approval:* AR, STB, ME, RS, ATE, MZ, AG, ED, FD, FC, ELZ, CO, JP, and PV.

ETHICAL APPROVAL RETROSPECTIVE STUDIES

This study was authorized by the French National Data Information and Freedom Commission (CNIL, reference number DE-2017–079) and the local ethics committee (CPP Ile-de-France 6, reference number n°2017-A02324–49, CPP/63–17). Patients consented to the extraction of data from their medical records.

DATA AVAILABILITY STATEMENT

Anonymized data will be shared on request from any qualified investigator.

ORCID

Albane Gareton https://orcid.org/0000-0002-3650-8581
Johan Pallud https://orcid.org/0000-0002-1652-9844

REFERENCES

1. Louis DN, Perry A, Reifenberger G, von Deimling A, Figarella-Branger D, Cavenee WK, et al. The 2016 World Health Organization Classification of Tumors of the Central Nervous System: a summary. Acta Neuropathol. 2016;131:803–20.
2. Molinaro AM, Taylor JW, Wiencke JK, Wrensch MR. Genetic and molecular epidemiology of adult diffuse glioma. Nat Rev Neurol. 2019;15:405–17.
3. Louis DN, Giannini C, Capper D, Paulus W, Figarella-Branger D, Lopes MB, et al. cIMPACT-NOW update 2: diagnostic clarifications for diffuse midline glioma, H3 K27M-mutant and diffuse astrocytoma/anaplastic astrocytoma, IDH-mutant. Acta Neuropathol. 2018;135:639–42.
4. Daumas-Duport C, Varlet P, Tucker ML, Beuvon F, Cervera P, Chodkiewicz JP. Oligodendrogliomas. Part I: patterns of growth, histological diagnosis, clinical and imaging correlations: a study of 153 cases. J Neurooncol. 1997;34:37–59.
5. Daumas-Duport C, Tucker ML, Kolles H, Cervera P, Beuvon F, Varlet P, et al. Oligodendrogliomas. Part II: A new grading system based on morphological and imaging criteria. J Neurooncol. 1997;34:61–78.
6. Pallud J, Capelle L, Taillandier L, Fontaine D, Mandonnet E, Guillevin R, et al. Prognostic significance of imaging contrast enhancement for WHO grade II gliomas. Neuro-Oncol. 2009;11:176–82.
7. Delfanti RL, Piccioni DE, Handwerker J, Bahrami N, Krishnan A, Karunamuni R, et al. Imaging correlates for the 2016 update on WHO classification of grade II/III gliomas: implications for IDH, 1p/19q and ATRX status. J Neurooncol. 2017;135:601–9.
8. Guo H, Kang H, Tong H, Du X, Liu H, Tan Y, et al. Microvascular characteristics of lower-grade diffuse gliomas: investigating vessel size imaging for differentiating grades and subtypes. Eur Radiol. 2019;29:1893–902.
9. Hempel J-M, Brendle C, Bender B, Bier G, Skardelly M, Gepfner-Tuma I, et al. Contrast enhancement predicting survival in integrated molecular subtypes of diffuse glioma: an observational cohort study. J Neurooncol. 2018;139:373–81.
10. Zhou H, Vallières M, Bai HX, Su C, Tang H, Oldridge D, et al. MRI features predict survival and molecular markers in diffuse lower-grade gliomas. Neuro-Oncology. 2017;19(6):862–70. https://academic.oup.com/neuro-oncology/article/19/6/862/2948265. Accessed 4 Apr 2020.
11. Bahrami N, Hartman SJ, Chang Y-H, Delfanti R, White NS, Karunamuni R, et al. Molecular classification of patients with grade II/III glioma using quantitative MRI characteristics. J Neurooncol. 2018;139:633–42.
12. Brat DJ, Aldape K, Colman H, Holland EC, Louis DN, Jenkins RB, et al. cIMPACT-NOW update 3: recommended diagnostic criteria for "Diffuse astrocytic glioma, IDH-wildtype, with molecular features of glioblastoma, WHO grade IV". Acta Neuropathol. 2018;136:805–10.
13. Louis DN, Ohgaki H, Wiestler OD, Cavenee WK, Burger PC, Jouvet A, et al. The 2007 WHO classification of tumours of the central nervous system. Acta Neuropathol. 2007;114:97–109.
14. Wen PY, Chang SM, Van den Bent MJ, Vogelbaum MA, Macdonald DR, Lee EQ. Response assessment in neuro-oncology clinical trials. J Clin Oncol. 2017;35(21):2439–49. https://www.ncbi.nlm.nih.gov/pmc/articles/PMC5516482/. Accessed 25 Jan 2020.
15. Roux A, Boddaert N, Grill J, Castel D, Zanello M, Zah-Bi G, et al. High prevalence of developmental venous anomaly in diffuse intrinsic pontine gliomas: a pediatric control study. Neurosurgery. 2020;86(4):517–23.
16. Roux A, Edjlali M, Porelli S, Tauziede-Espariat A, Zanello M, Dezamis E, et al. Developmental venous anomaly in adult patients with diffuse glioma: a clinically relevant coexistence? Neurology. 2019;92:e55–e62.
17. Reuss DE, Sahm F, Schrimpf D, Wiestler B, Capper D, Koelsche C, et al. ATRX and IDH1-R132H immunohistochemistry with subsequent copy number analysis and IDH sequencing as a basis for an "integrated" diagnostic approach for adult astrocytoma, oligodendroglioma and glioblastoma. Acta Neuropathol. 2015;129:133–46.
18. Ideguchi M, Kajiwara K, Goto H, Sugimoto K, Nomura S, Ikeda E, et al. MRI findings and pathological features in early-stage glioblastoma. J Neurooncol. 2015;123:289–97.
19. Tihan T, Vohra P, Berger MS, Keles GE. Definition and diagnostic implications of gemistocytic astrocytomas: a pathological perspective. J Neurooncol. 2006;76:175–83.
20. Louis DN, Perry A, Burger P, Ellison DW, Reifenberger G, von Deimling A, et al. International Society of Neuropathology-Haarlem consensus guidelines for nervous system tumor classification and grading. Brain Pathol Zurich Switz. 2014;24:429–35.
21. Juratli TA, Tummala SS, Riedl A, Daubner D, Hennig S, Penson T, et al. Radiographic assessment of contrast enhancement and T2/FLAIR mismatch sign in lower grade gliomas: correlation with molecular groups. J Neurooncol. 2019;141:327–35.
22. Wang YY, Wang K, Li SW, Wang JF, Ma J, Jiang T, et al. Patterns of tumor contrast enhancement predict the prognosis of anaplastic gliomas with IDH1 mutation. AJNR Am J Neuroradiol. 2015;36:2023–9.
23. Hasselblatt M, Jaber M, Reuss D, Grauer O, Bibo A, Terwey S, et al. Diffuse astrocytoma, IDH-wildtype: a dissolving diagnosis. J Neuropathol Exp Neurol. 2018;77(6):422–5.
24. Bale TA, Jordan JT, Rapalino O, Ramamurthy N, Jessop N, DeWitt JC, et al. Financially effective test algorithm to identify

an aggressive, EGFR-amplified variant of IDH-wildtype, lower-grade diffuse glioma. Neuro-Oncol. 2019;21:596–605.
25. Faguer R, Tanguy J-Y, Rousseau A, Clavreul A, Menei P. Early presentation of primary glioblastoma. Neurochirurgie. 2014;60:188–93.
26. Hishii M, Matsumoto T, Arai H. Diagnosis and treatment of early-stage glioblastoma. Asian J Neurosurg. 2019;14:589–92.
27. Papadopoulos MC, Saadoun S, Woodrow CJ, Davies DC, Costa-Martins P, Moss RF, et al. Occludin expression in microvessels of neoplastic and non-neoplastic human brain. Neuropathol Appl Neurobiol. 2001;27:384–95.
28. Wolburg H, Wolburg-Buchholz K, Kraus J, Rascher-Eggstein G, Liebner S, Hamm S, et al. Localization of claudin-3 in tight junctions of the blood-brain barrier is selectively lost during experimental autoimmune encephalomyelitis and human glioblastoma multiforme. Acta Neuropathol. 2003;105:586–92.

SUPPORTING INFORMATION

Additional supporting information may be found online in the Supporting Information section.

FIGURE S1 Histo-radiological consensus evaluation illustration. Left: Contrast-enhanced 3D T1 FSPGR sequence showing a ring-like tumor located in the left lenticular nuclei with a peripheral hypo-signal. Right: Hematoxylin Phloxine Saffron stains showing an image guided tissue sampling performed in the peripheral hypo-signal (superior) or in the ring-like component (middle and inferior)

FIGURE S2 Diagnosis and grade changes from 2007 WHO to 2016 WHO Classification. *2007 WHO Classification*. AII: grade 2, diffuse astrocytoma; AIII: grade 3, anaplastic astrocytoma; OAII : grade 2, oligo-astrocytoma; OAIII: grade 3, anaplastic oligo-astrocytoma; OII: grade 2, oligodendroglioma; OIII: grade 3, anaplastic oligodendroglioma; GBM: grade 4, glioblastoma; GBMo: grade 4, *glioblastoma* with oligodendroglioma component; GBM-PNET: grade 4, *glioblastoma* with primitive neuroectodermal tumor-like component; GC-GBM: grade 4, giant cells glioblastoma; and GS: grade 4, gliosarcoma. *2016 WHO Classification*. AII-*IDH*mut: grade 2, diffuse astrocytoma, *IDH*-mutant; AII-*IDH*wt: grade 2, diffuse astrocytoma, *IDH*-wild type; AIII-*IDH*mut: grade 3, anaplastic astrocytoma, *IDH*-mutant; AIII-*IDH*wt: grade 3, anaplastic astrocytoma, *IDH*-wild type; OII: grade 2, oligodendroglioma, *IDH*-mutant and 1p/19q-codeleted; OIII: grade 3, anaplastic oligodendroglioma, *IDH*-mutant and 1p/19q-codeleted; DMG: grade 4, diffuse midline glioma, *H3K27M*-mutant; GBM-*IDH*mut: grade 4, glioblastoma, *IDH*-mutant; GBM-*IDH*wt: grade 4, glioblastoma, *IDH*-wild type; GC-GBM: grade 4, giant cells glioblastoma, *IDH*-wild type; GS: grade 4, gliosarcoma, *IDH*-wild type; GBME: grade 4, epithelioid glioblastoma, *IDH*-wild type

Figure S3 Diagnosis and grade changes from 2016 WHO Classification to 2016 WHO Classification with cIMPACT-NOW updates. *2016 WHO Classification*. AII-*IDH*mut: grade 2, diffuse astrocytoma, *IDH*-mutant; AII-*IDH*wt: grade 2, diffuse astrocytoma, *IDH*-wild type; AIII-*IDH*mut: grade 3, anaplastic astrocytoma, *IDH*-mutant; AIII-*IDH*wt: grade 3, anaplastic astrocytoma, *IDH*-wild type; OII: grade 2, oligodendroglioma, *IDH*-mutant and 1p/19q-codeleted; OIII: grade 3, anaplastic oligodendroglioma, *IDH*-mutant and 1p/19q-codeleted; DMG: grade 4, diffuse midline glioma, *H3K27M*-mutant; GBM-*IDH*mut: grade 4, glioblastoma, *IDH*-mutant; GBM-*IDH*wt: grade 4, glioblastoma, *IDH*-wild type; GC-GBM: grade 4, giant cells glioblastoma, *IDH*-wild type; GS: grade 4, gliosarcoma, *IDH*-wild type; GBME: grade 4, epithelioid glioblastoma, *IDH*-wild type. *WHO 2016 with cIMPACT-NOW updates*. GBM-mol: diffuse astrocytic glioma, *IDH*-wild type, with molecular features of glioblastoma

FIGURE S4 Survival analyses. The color legend is similar to Figures 4, 5 and Figure S3

TABLE S1 Main characteristics of the study sample (n = 679)

How to cite this article: Roux A, Tran S, Edjlali M, et al. Prognostic relevance of adding MRI data to WHO 2016 and cIMPACT-NOW updates for diffuse astrocytic tumors in adults. Working toward the extended use of MRI data in integrated glioma diagnosis. *Brain Pathology*. 2021;31:e12929. https://doi.org/10.1111/bpa.12929